Supporting Information

$CoSe_2$ anchored vertical graphene/macroporous carbon nanofibers as multifunctional interlayer for high-performance lithium-sulfur batteries

Yangcheng Mo, Kaochun Yang, Junsheng Lin, Mengting Liu, Guanfei Ye, Jie Yu*

Guangdong Provincial Key Laboratory of Semiconductor Optoelectronic Materials and Intelligent Photonic Systems, Shenzhen Engineering Lab for Supercapacitor Materials, School of Material Science and Engineering, Harbin Institute of Technology, Shenzhen, University Town, Shenzhen 518055, China.

* Corresponding author

E-mail address: jyu@hit.edu.cn

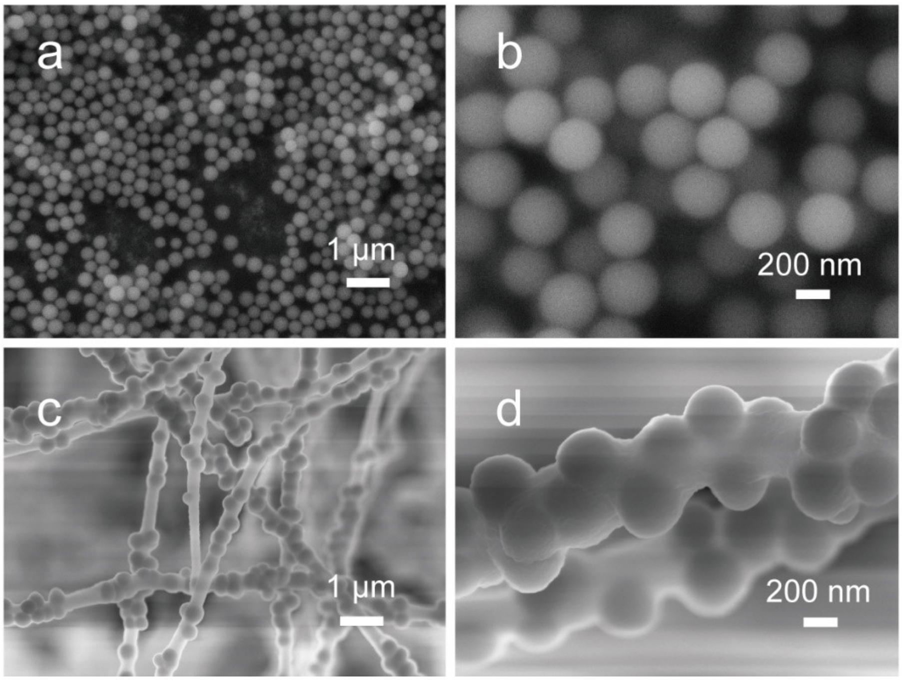

Figure S1 SEM images of (a), (b) SiO_2 sphere and (c), (d) SiO_2@PAN.

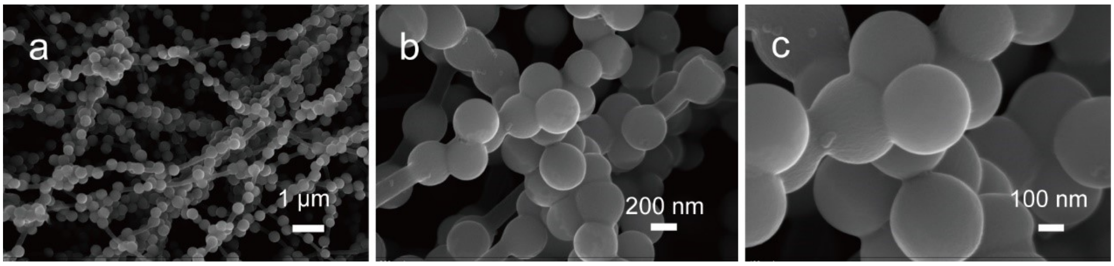

Figure S2 SEM images of SiO_2@C fibers at different magnification.

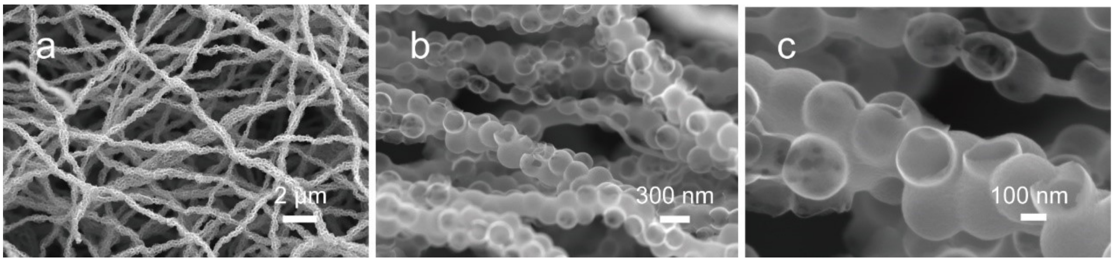

Figure S3 SEM images of MFs at different magnification.

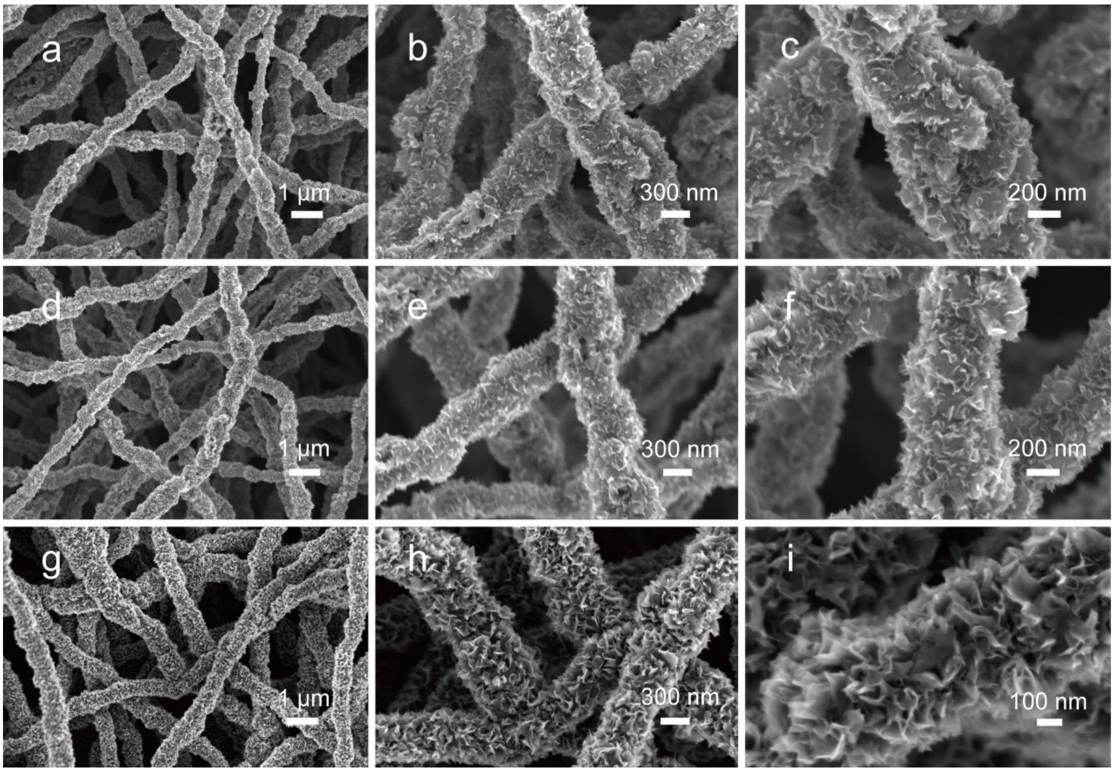

Figure S4 SEM images of the VGMFs growth for different time. (a-c) 1 h, (b-f) 2.5 h, (g-i) 4 h.

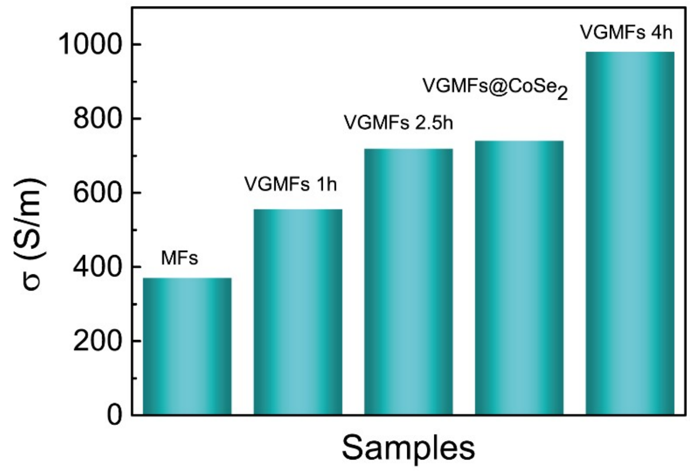

Figure S5 The electrical conductivity of the VGMFs grown for different time.

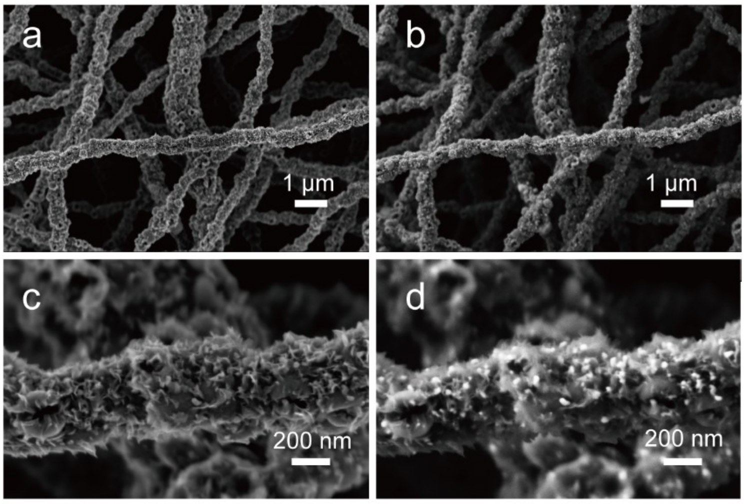

Figure S6 SEM images of the VGMFs@$CoSe_2$ under different signals. (a), (c) based on the signal of Inlens, (b), (d) based on the signal of SE2.

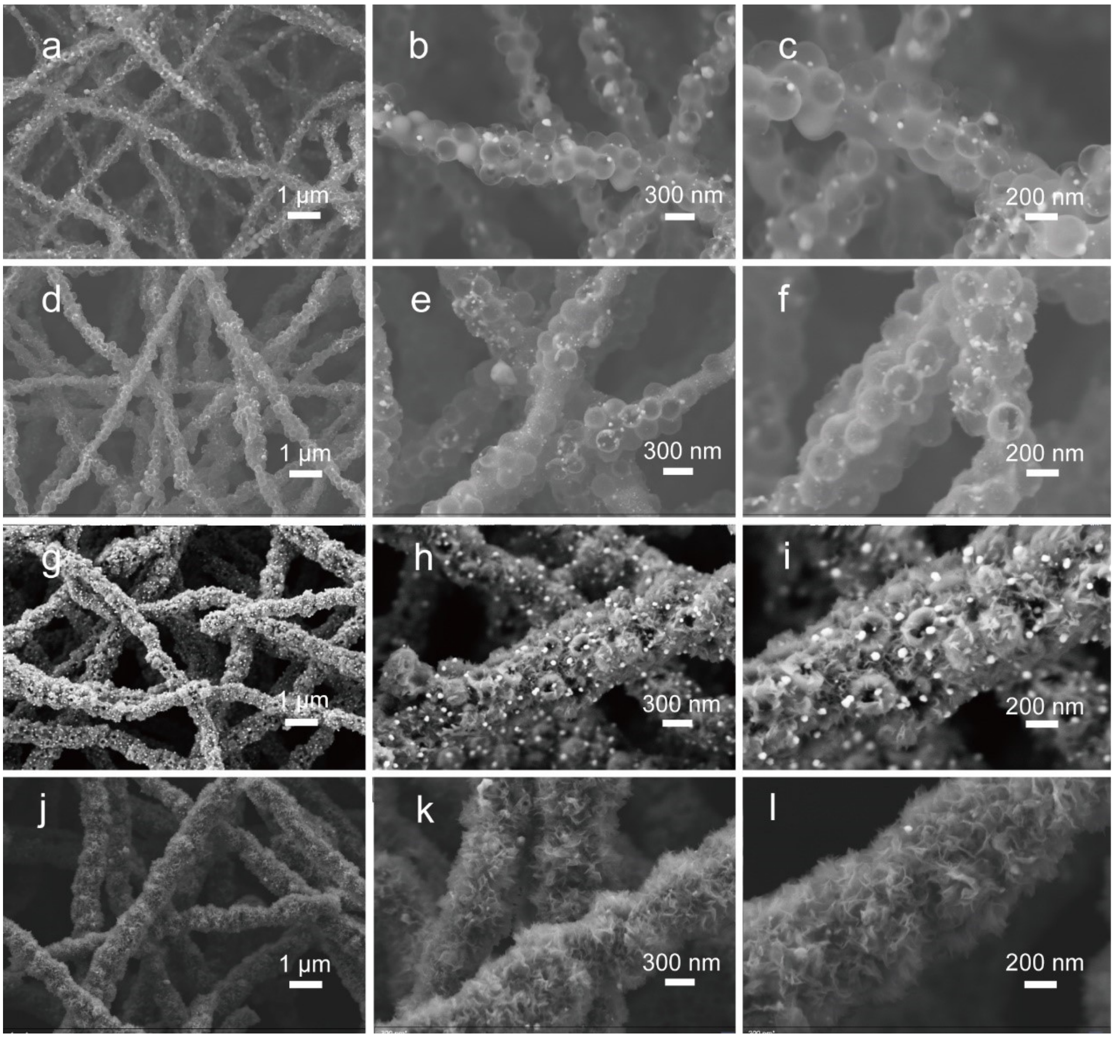

Figure S7 SEM images of the VGMFs@$CoSe_2$ for different growth time of VGs. (a)-(c) 0 h, (d)-(f) 1 h, (g)-(i) 2.5 h, (j)-(l) 4 h.

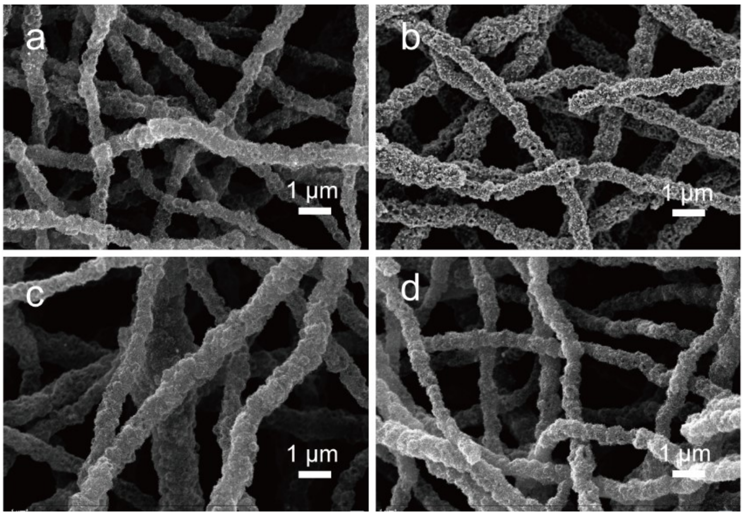

Figure S8 SEM images of the VGMFs@$CoSe_2$ for different selenizing temperature, (a) 300 °C, 450 °C, (C) 525 °C, 600 °C.

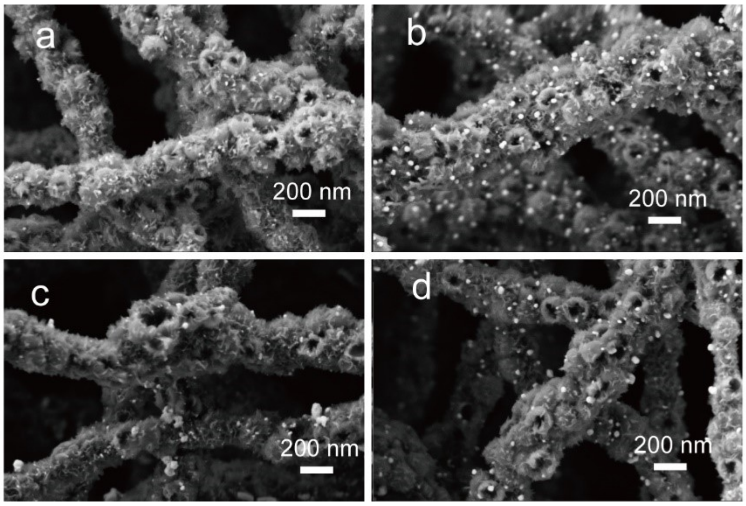

Figure S9 SEM images of the VGMFs@$CoSe_2$ for different molar concentration of $Co(NO_3)_2 \cdot 6H_2O$, (a) 0.025 M, 0.05 M, (C) 0.1 M, (D) 0.2 M.

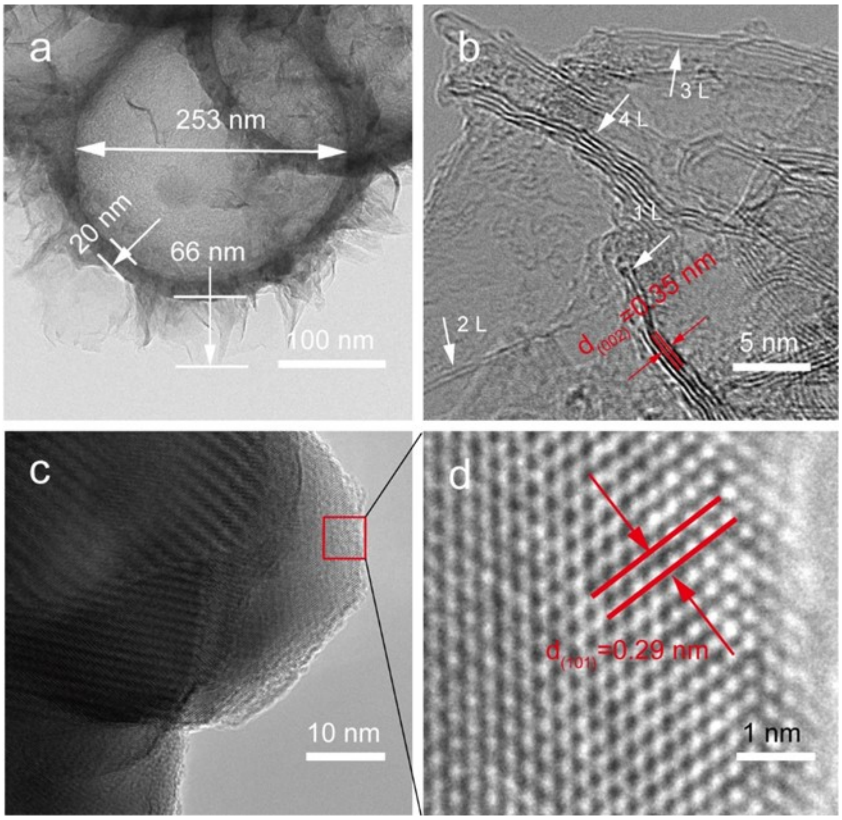

Figure S10 TEM images of the VGMFs@$CoSe_2$. (a) the pore size, the carbon shell of macropore, and the thickness of the VGs. (b) edge structure of the VGs, (c), (d) HRTEM image of $CoSe_2$.

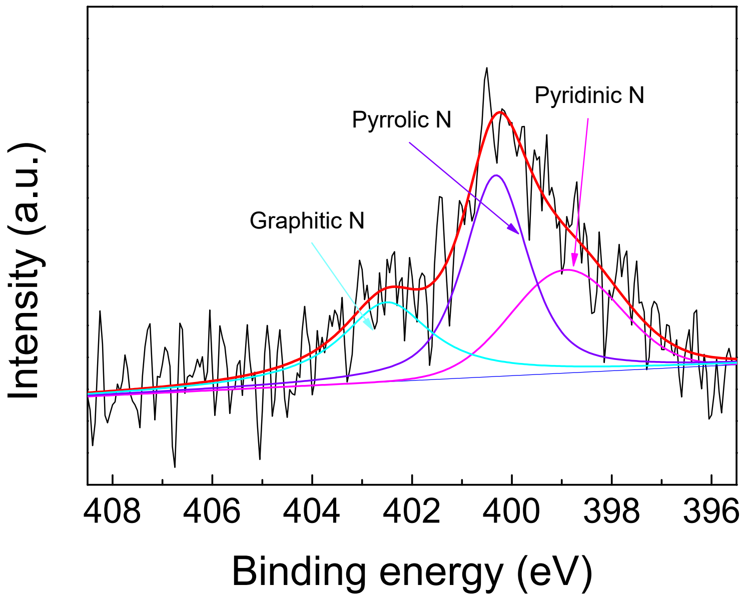

Figure S11 The N 1s spectrum of VGMFs@$CoSe_2$.

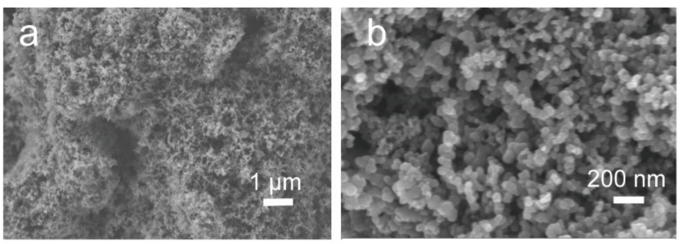

Figure S12 SEM images of sulfur electrodes.

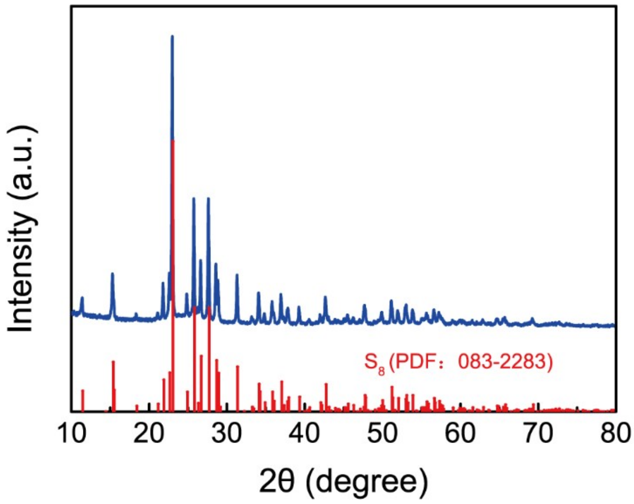

Figure S13 XRD pattern of the sulfur electrodes.

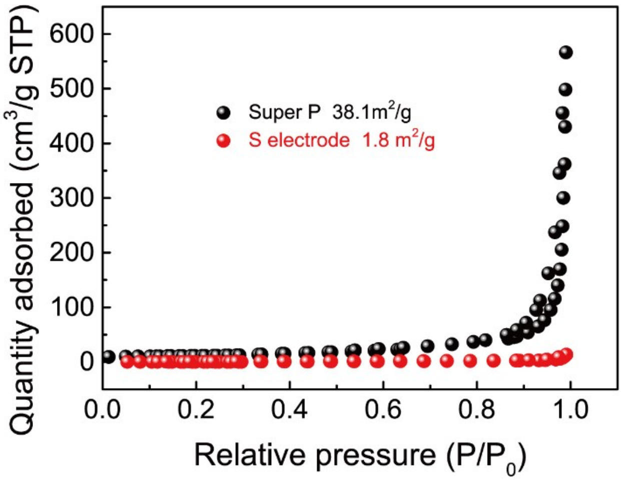

Figure S14 N_2 adsorption/desorption isotherms of the super P and sulfur electrodes, respectively.

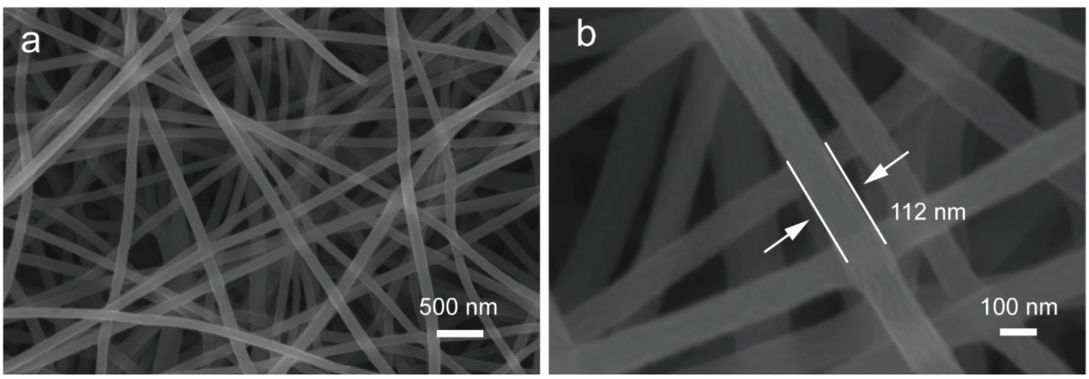

Figure S15 SEM images of CNFs.

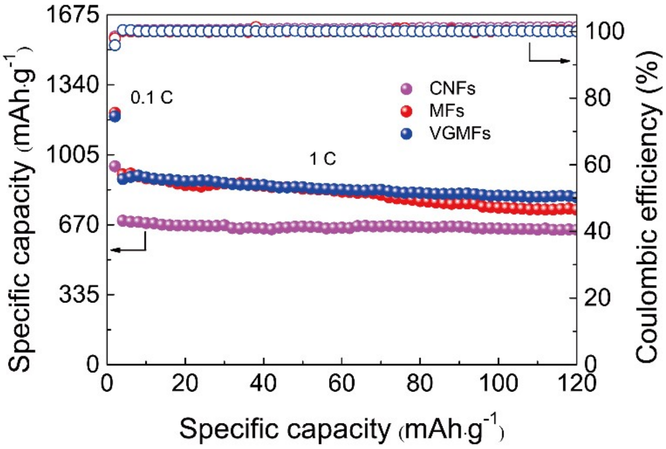

Figure S16 The cycling performance of the batteries with different interlayers of CNFs, MFs and VGMFs.

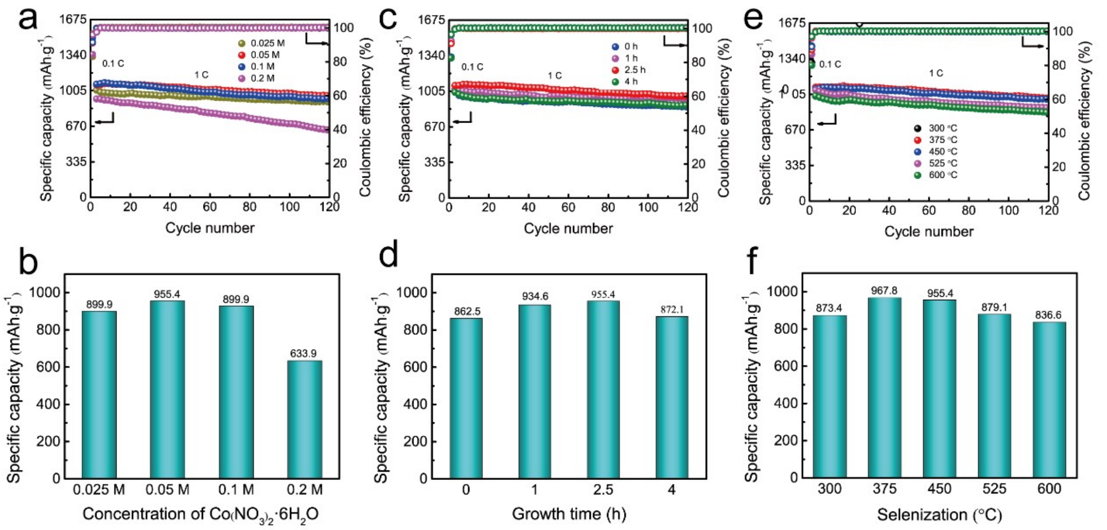

Figure S17 The cycle performance and the capacities after 120 cycles under experimental parameters, respectively. (a), (b) different molar concentration of cobalt nitrate hexahydrate, (c), (d) different growth time of VGs, (e), (f) different selenization temperatures.

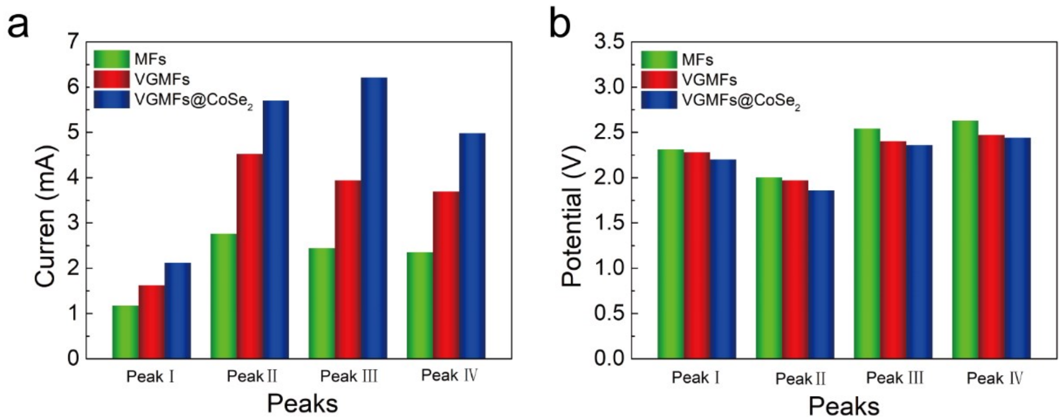

Figure S18 The current and potential intensity of each peak from CV curves of the batteries with different interlayers.

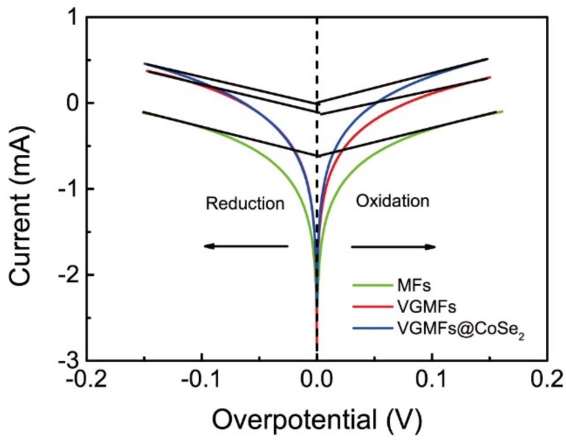

Figure S19 Tafel curves of symmetric batteries of the batteries with various interlayers.

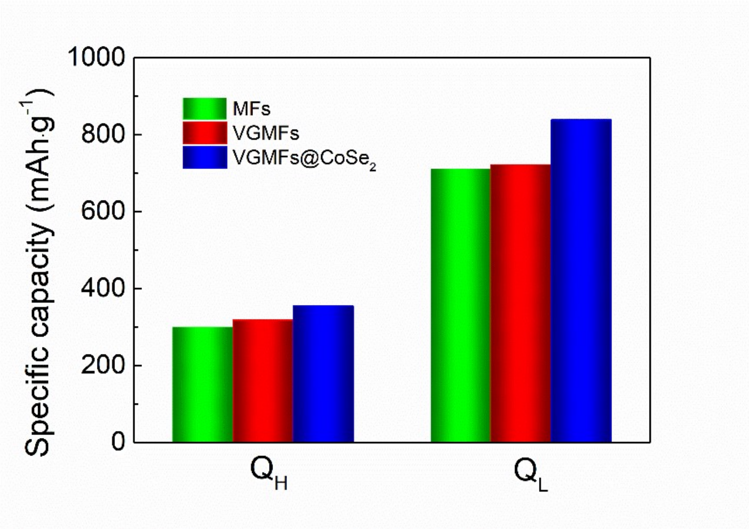

Figure S20 The capacities of the batteries on high (Q_H) and low (Q_L) potential plateau.

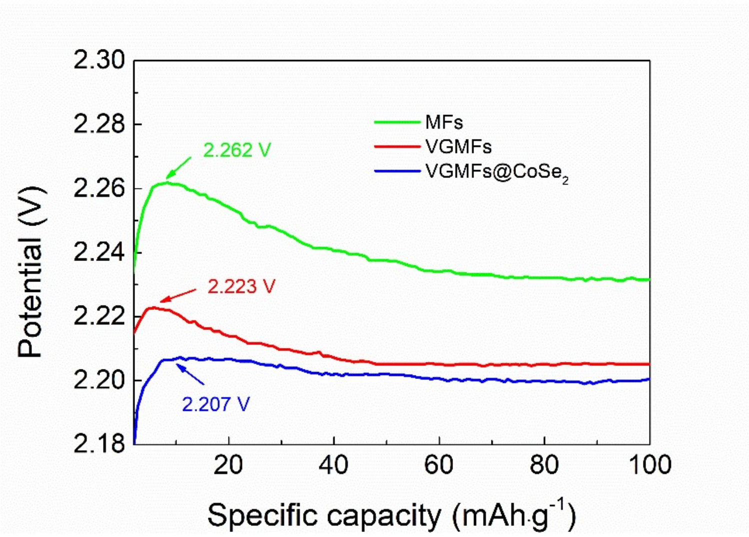

Figure S21 Charge curves comparison of the batteries with different interlayers.

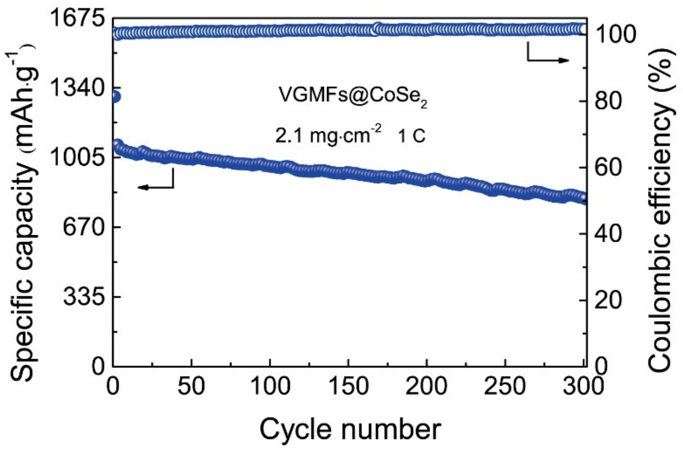

Figure S22 Long-term cycling of the battery containing VGMFs@$CoSe_2$ interlayer with a sulfur loading of 2.1 $mg\cdot cm^{-2}$.

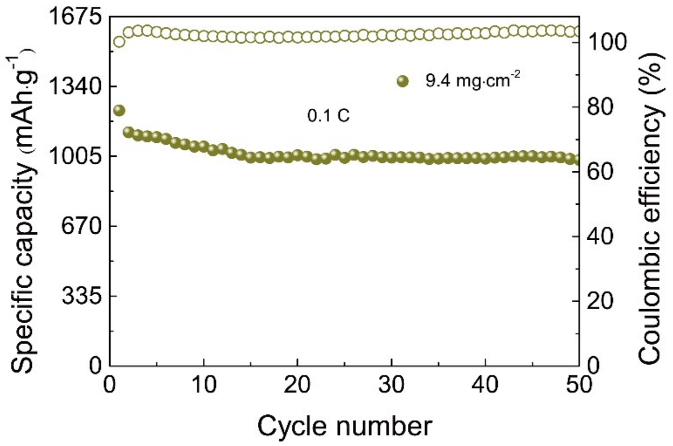

Figure S23 Electrochemical performance with a sulfur loading of 9.4 $mg\cdot cm^{-2}$.

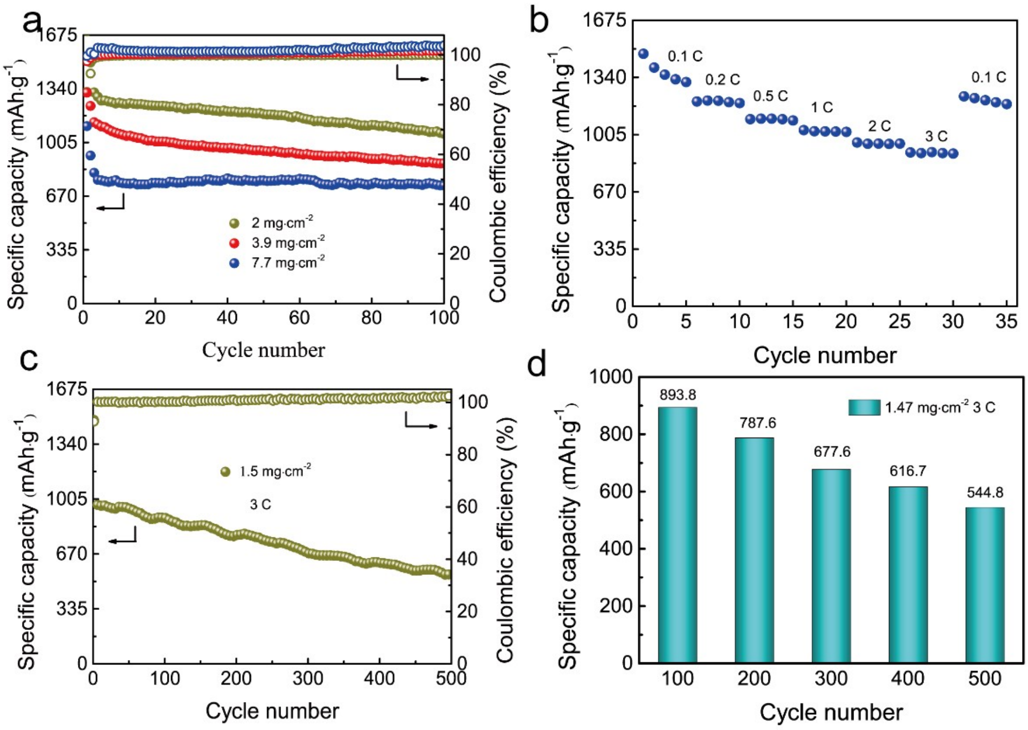

Figure S24 Electrochemical performance of the batteries with VGMFs@$CoSe_2$ interlayer prepared at 450 °C.

Table S1 The main parameters of the batteries with different interlayers

Interlayers	Sulfur loading ($mg \cdot cm^{-2}$)	E/S ratio ($\mu L \cdot mg^{-1}$)	Rate (C).
MFs	2	30	1
VGMFs	2	30	1
VGMFs@$CoSe_2$	2	30	1
VGMFs@$CoSe_2$	2.4	26.3	0.2
VGMFs@$CoSe_2$	5.2	11.9	0.2
VGMFs@$CoSe_2$	8.5	7.4	0.2
VGMFs@$CoSe_2$	9.4	6.7	0.1

\

Table S2 Electrochemical performances of our work compared with previous works.

Samples	Rate capacity	Performance at high sulfur loading	Refs.
NbN@NG	819 mAh·g^{-1} (4 C)	4.5 mg·cm^{-2} at 0.5 C (807 mAh·g^{-1} after 300th cycle)	[1]
Mn_2P@C/carbon paper	659.7 mAh·g^{-1} (5 C)	5.4 mg·cm^{-2} at 0.5 C (551.3 mAh·g^{-1} at 140th cycle)	[2]
$Se_{0.06}$SPAN/MMT	905.5 mAh·g^{-1} (2 C)	6.96 mg·cm^{-2} at 0.1 C (849.1 mAh·g^{-1} at 60th cycle)	[3]
CoFe/NHCS	1029 mAh·g^{-1} (2 C)	6.7 mg·cm^{-2} at 0.1 C (671.6 mAh·g^{-1} at 100th cycle)	[4]
Mo_2N@NG	860.2 mAh·g^{-1} (4 C)	3.6 mg·cm^{-2} at 0.5 C (558.2 mAh·g^{-1} at 300th cycle)	[5]
MMT/RGO-PP	848 mAh·g^{-1} (3 C)	6.8 mg·cm^{-2} at 0.1 C (4.95 mAh·cm^{-2} at 40th cycle)	[6]
MoS_{2-x}-Co_9S_{8-y}/rGO	710.2 mAh·g^{-1} (3 C)	4.8 mg·cm^{-2} at 0.2 C (3.55 mAh·cm^{-2} at 100th cycle)	[7]
In_2O_{3-x}@CS-0.6/rGO	872 mAh·g^{-1} (3 C)	6.81 mg·cm^{-2} at 0.2 C (6.98 mAh·cm^{-2} at 50th cycle)	[8]
Ni-Co-P@C	654.5 mAh·g^{-1} (5 C)	3 mg·cm^{-2} at 0.2 C (3.7 mAh·cm^{-2} at 85th cycle)	[9]
C-Lepidolite@PP	703 mAh·g^{-1} (7 C)	8.45 mg·cm^{-2} at 0.2 C (<5.72 mAh·cm^{-2} within 50 cycles)	[10]
VGMFs@$CoSe_2$	917.7 mAh·g^{-1} (3 C)	8.5 mg·cm^{-2} at 0.2 C (6.9 mAh·cm^{-2} or 806.1 mAh·g^{-1} at 120th cycle) 9.4 mg·cm^{-2} at 0.1 C (average10.1 mAh·cm^{-2} or 1022 mAh·g^{-1} within 50 cycles.)	This work

References

[1] F. Ma, X. Zhang, K. Sriniva, D. Liu, Z. Zhang, X. Chen, W. Zhang, Q. Wu, Y. Chen, J. Mater. Chem. A, 2022, 10, 8578.

[2] H. Yang, M. Geng, W. Tang, C. Shang, Chem. Eng. J., 2022, 450, 137925.

[3] W. Wang, K. Xi, B. Li, H. Li, S. Liu, J. Wang, H. Zhao, H. Li, A.M. Abdelkader, X. Gao, G. Li, Adv. Energy Mater., 2022, 12 2200160.

[4] Z. Gu, C. Cheng, T. Yan, G. Liu, J. Jiang, J. Mao, K. Dai, J. Li, J. Wu, L. Zhang, Nano Energy, 2021, 86, 106111.

[5] F. Ma, K. Srinivas, X. Zhang, Z. Zhang, Y. Wu, D. Liu, W. Zhang, Q. Wu, Y. Chen, Adv. Funct. Mater., 2022, 32, 2206113.

[6] X. Long, Z.-H. Luo, W.-H. Zhou, S.-K. Zhu, Y. Song, H. Li, C.-N. Geng, B. Shi, Z.-Y. Han, G.-M. Zhou, W. Lv, J.-J. Shao, Energy Storage Mater., 2022, 52, 120-129.

[7] H. Song, T. Li, T. He, Z. Wang, D. Fang, Y. Wang, X. L. Li, D. Zhang, J. Hu, S. Huang, Chem. Eng. J., 2022, 450, 138115.

[8] K. Zou, X. Chen, W. Jing, X. Dai, P. Wang, Y. Liu, R. Qiao, M. Shi, Y. Chen, J. Sun, Y. Liu, Energy Storage Mater., 2022, 48, 133-144.

[9] Z. Wu, S. Chen, L. Wang, Q. Deng, Z. Zeng, J. Wang, S. Deng, Energy Storage Mater., 2021, 38, 381-388.

[10] G. Zeng, Y. Liu, D. Chen, C. Zhen, Y. Han, W. He, Adv. Energy Mater., 2021, 11, 2102058.